ORIGINAL ARTICLE

WILEY

Local tumour response to neoadjuvant therapy with 2-aminoethyl dihydrogen phosphate in dogs with soft tissue sarcoma

Patrícia Ferreira de Castro[1] 🔵 | Durvanei Augusto Maria[2] |
Ana Carolina Brandão de Campos Fonseca Pinto[1] | Geni Cristina Fonseca Patricio[1] |
Julia Maria Matera[1]

[1] Department of Surgery, School of Veterinary Medicine and Animal Science, University of São Paulo, São Paulo, Brazil

[2] Development and Innovation Laboratory, Butantan Institute, São Paulo, Brazil

Correspondence
Patrícia Ferreira de Castro, Department of Surgery, School of Veterinary Medicine and Animal Science, University of São Paulo, São Paulo, Brazil.
Email: pfcastro@usp.br

[Correction added on 24 March 2022, after first online publication: The third author's name was corrected to "Ana Carolina Brandão de Campos Fonseca Pinto".]

Abstract

Background: In cases of soft tissue sarcoma (STS), neoadjuvant therapy is indicated to downstage the tumour prior to surgery to achieve enhanced local tumour control. The antineoplastic phospholipid compound 2-aminoethyl dihydrogen phosphate (2-AEH2F) is an alkyl phosphate ester capable of inhibiting cell proliferation and inducing cell death by modifying the asymmetry of phospholipids in the cytoplasmic membrane

Objectives: This clinical study was designed to investigate local antitumoural effects of neoadjuvant therapy with 2-AEH2F in dogs with naturally occurring STS

Material and methods: Dogs ($n = 11$) received four consecutive weekly intravenous injections of 2-AEH2F (70 mg/kg) prior to tumour resection. Tomographic (CT) and thermal (TE) images were used to investigate changes in tumour size and local temperature in response to treatment

Results: Comparative analysis of CT images ($n = 9/11$) failed to reveal complete or partial remission according to selected assessment criteria (RECIST, WHO and volumetric). Comparative analysis of TE images ($n = 10/11$) revealed significantly ($p = 0.01416$) lower temperatures in tumoural areas relative to surrounding tissues over the course of treatment

Conclusions: 2-AEH2F had no cytoreductive effects when used at doses and intervals described in this study. However, significant drop in skin temperatures recorded in tumoural areas suggest induction of physiological changes.

KEYWORDS
antineoplastic phospholipid, dog, local tumour, neoadjuvant therapy, soft tissue sarcoma, thermal images

1 | INTRODUCTION

Soft tissue sarcomas (STS) are a group of tumours of mesenchymal origin with different histologic grade (Dennis et al., 2011; Dernell et al., 1998; Ehrhart, 2005). These tumours have been described in human and veterinary patients and are estimated to account for 9 to 15% of skin and subcutaneous tumours in dogs (Dennis et al., 2011; Ehrhart, 2005; Liptak & Christensen, 2019). Soft tissue sarcomas have a soft or firm pseudo capsule with poorly demarcated margins and often infiltrate deeper tissues. Despite low to moderate metastatic potential, these features are associated with local invasiveness and high rates of local recurrence. Therefore, depending on size of mass and anatomic location, surgery with wide margins or amputation of extremities is the treatment of choice in most cases (Dernell et al., 1998; Liptak & Christensen, 2019; Mauldin, 1997; Thrall & Gillette, 1995).

Neoadjuvant therapy could be indicated in STS to downstage the tumour prior to surgery in efforts to achieve enhanced local tumour control. Downstaging strategies are aimed at inducing tumour shrinkage and making tumours less firmly attached and less invasive. The goal of neoadjuvant treatment for STS is to destroy tumoural tissues by targeting tumour vessels or cells (Hohenberger & Wysocki, 2008). Brock, in 1959, was the first to report the benefits of preoperative chemotherapy with cyclophosphamide for tumour treatment in rats (Brock, 1959). However, the term *neoadjuvant* therapy was introduced by Frei in 1982 to designate chemotherapeutic strategies for non-resectable primary solid tumours (Frei, 1982).

In human patients with STS systemic treatment with doxorubicin and/or ifosfamide may induce cytoreduction in up to 30% of cases (Komdeur et al., 2002). However, conventional chemotherapy is associated with severe systemic side effects, and there are no effective alternatives to doxorubicin and ifosfamide (Hohenberger & Wysocki, 2008). The role of chemotherapy in treatment of canine STS has not been well established with historically poor responses of gross tumour in canine STS to standard conventional chemotherapeutic agents (Liptak & Christensen, 2019; Selting, 2010). Novel therapies are currently changing treatment algorithms for advanced carcinomas and melanomas and similar approaches are being applied in sarcoma research (Borgatti et al., 2020), making room for in vivo studies of new systemic therapies in addition to conventional drugs.

Different from conventional chemotherapeutic agents, the phospholipid 2-AEH2F induces cell death by modifying the cytoplasmic membrane rather than the DNA. Among other mechanisms of action, 2-AEH2F internalisation via endocytosis mediated by lipid-rafts (lipid microdomain receptors) has been proposed (Van Der Luit et al., 2003; Van Der Luit et al., 2007). At the membrane level, lipid-rafts interfere with phospholipid turnover and may alter the physical properties of cell membranes and affect the generation of second messengers such as phosphatidic acid, diacylglycerol and phosphoinositide, leading to cell stress and apoptosis (Sprong et al., 2001; Van Blitterswijk & Verheij, 2013).

Studies investigating novel pathways for synthesis of 2-aminoethyl dihydrogen phosphate (2-AEH2F) conducted at *Development and Innovation Laboratory, Butantan Institute* revealed high cytotoxic potential of this compound against different tumour cell lines, such as B16F10 (murine melanoma), EAT (Ehrlich ascites tumour), Renca (murine renal cell carcinoma) and MCF-7 (human mammary adenocarcinoma), with no negative impacts on the proliferative capacity of normal cells (Ferreira, Freitas et al., 2013; Ferreira et al., 2011; Ferreira, Meneguelo, Marques et al., 2012; Ferreira, Meneguelo et al., 2013; Ferreira, Meneguelo, Pereira et al., 2012; Luna et al., 2014; Meneguelo, 2007). The potential of 2-AEH2F to induce tumour shrinkage has been demonstrated in in vivo studies in mice with melanoma (Ferreira et al., 2011; Veronez, 2012).

To further investigate the applicability of 2-AEH2F as an antineoplastic agent, a prospective clinical study in dogs with naturally occurring STS was designed. Dogs in this study received combined treatment with 2-AEH2F and surgical resection (Castro, 2019). Major benefits of preoperative chemotherapy include in vivo assessment of response to treatment based on changes in tumour size and/or imaging characteristics (Lucas et al., 2008). In this study, assessment of local tumour response to neoadjuvant therapy with 2-AEH2F was based on computed tomographic (CT) and thermal (TE) imaging of regions of interest in treated dogs.

2 | MATERIAL AND METHODS

This study was approved by the Ethics Committee on Animal Use (CEUA) of the School of Veterinary Medicine and Animal Science of the University of São Paulo (Protocol: 3495130715/2015).

2.1 | Patients

Dogs with cutaneous and/or subcutaneous mesenchymal tumours diagnosed by cytology were included in this prospective clinical study. Patients with suspected metastatic disease on thoracic radiograph or abdominal ultrasound images and patients whose histopathological diagnosis after tumour removal did not confirm that they were STS were excluded.

2.2 | Chemotherapeutic agent

In this research project, 2-AEH2F chemical synthesis was based on the esterification under pressure and controlled vacuum of phosphoric acid to ethanolamine. The quality and purity of 2-AEH2F was analysed in plasma by inductive coupling and mass spectrometry. The process is based on the ionisation of a sample by an extremely hot plasma, usually made from argon gas. The results obtained showed product with a degree of purity of esterified monophosphoester higher than 97.8%. Stock solution (1 M) was diluted in water (pH 7.2), stored at 4°C temperature, diluted in sterile phosphate saline and filtrated in sterile 0.22 μm membrane (De Almeida Leitão Da Cunha et al., 2021).

2.3 | Experimental design

Neoadjuvant therapy consisted of weekly intravenous (IV) administration of 70 mg/kg of 2-AEH2F diluted in 100 ml of sterile 0.9 % saline at a rate of 10 ml/kg/h. Dogs were treated for four consecutive weeks (T_0–T_3) and submitted to surgical resection (T_4). To evaluate local tumour response in dogs to instituted therapy, CT and TE images of the region of interest were obtained as follows:

- CT images acquired prior to (T_0) and after completion of preoperative neoadjuvant therapy immediately before the surgical procedure (T_4).
- TE images collected prior first application of neoadjuvant therapy (T_0), each application of 2-AEH2F (T_1–T_3) and the surgical procedure (T_4).

Before each application of 2-AEH2F, physical and laboratory examinations (complete blood count, renal profile, liver profile) were performed. Patients were monitored for vital signs (temperature, respiratory rate and pulse) during the infusion and evaluated against the Common Terminology Criteria for Adverse Events following chemotherapy or biological antineoplastic therapy in dogs and cats from the Veterinary Cooperative Oncology Group (VCOG-CTCAE) (VCOG, 2016). Adverse events considered for the period between T_0 and T_4: anaemia, neutropenia, thrombocytopenia, liver toxicity (alanine aminotransferase and alkaline phosphatase), renal toxicity (creatinine), anorexia, emesis and diarrhoea.

2.4 | Tomographic imaging

Tomographic images were obtained using a multi-slice helical CT scanner with 16 channels (Philips MX 8000 IDT). Dogs were scanned under general anaesthesia and positioned as needed to prevent tumour compression and changes in tumour shape. Plain and contrast-enhanced images were acquired consecutively. Contrast-enhancement was achieved with intravenous bolus injection of 1.5 ml/kg of iodinated water-soluble contrast agent (Omnipaque® ioexol, 300 mg I/ml, GE Healthcare, Shanghai Co., Ltd, China) via a peripheral vein. Image acquisition parameters were as follows: 120 kVp, 150–240 mAs and 2–3 mm slice thickness.

Tomographic images were analysed using Osirix software. The following measurements were made: largest tumour cross-sectional diameter (one-dimensional), product of the largest tumour diameter and its maximum perpendicular diameter (two-dimensional) and volume (three-dimensional; obtained using the 'ROI volume' tool). Measurements were made from tumoural areas demarcated in cross-sectional CT slices.

2.5 | Thermal imaging

Thermal images of tumours in this sample were acquired using a FLIR T650sc infrared camera (FLIR Systems, Inc.). Images were acquired with standardised camera-to-object distance (0.5 m) in an indoor environment with no drafts. The area of interest was shaved 15 minutes prior to image acquisition.

Thermal images were analysed using software (Flir R Research; FLIR Systems, Inc.). Temperature measurements were collected at the following sites:

- point located at the centre of the tumour (TP);
- point located on healthy tissue close to the tumour (non-tumoural point, NTP);
- elliptical or circular-shaped area surrounding and encompassing the TP (tumoural area, TA);
- elliptical or circular-shaped area of similar size to TA surrounding the NTP (non-tumoural area, NTA; small differences between TA and NTA could not be avoided due to anatomical location and size of tumours in some cases).

2.6 | Tumour response assessment criteria

Tomographic parameters recorded prior to and after neoadjuvant therapy with 2-AEH2F were assessed as follows:

- One-dimensional – tumour size according to Response Evaluation Criteria in Solid Tumours (RECIST) (Therasse et al., 2000).
- Two-dimensional – tumour size according to World Health Organization (WHO) criteria (Miller et al., 1981).
- Three-dimensional – tumour volume according to the volumetric criterion (VOL) (Chappell et al., 1998).

Changes in tumour size (%) were calculated using the following equation:

$$\text{Change in tumor size\%} = \frac{(\text{tumor size at } T_4 - \text{tumor size at } T_0) \times 100}{\text{tumor size at } T_0}$$

RECIST, WHO and VOL assign four categories of response (Grabellus et al., 2012):

- RECIST: resolution of lesion (complete response = CR), tumour size reduction $\geq 30\%$ (partial response = PR), tumour size increase $\geq 20\%$ (progressive disease = PD), change in tumour size between PR and PD (stable disease = SD). In this study, tumour size reduction $\geq 30\%$ (CR or PR) between T_0 and T_4 was defined as 'response with cytoreduction'.
- WHO: resolution of lesion (complete response = CR), tumour size reduction $\geq 50\%$ (partial response = PR), tumour size increase $\geq 25\%$ (progressive disease = PD), absence of PR or PD – that is, no change (stable disease = SD). In this study, tumour size reduction $\geq 50\%$ (CR or PR) between T_0 and T_4 was defined as 'response with cytoreduction'.
- VOL: resolution of lesion (complete response = CR), tumour size reduction $\geq 65\%$ (partial response = PR), tumour size increase ≥ 40

(progressive disease = PD), absence of PR or PD – that is, no change (stable disease = SD). In this study, tumour size reduction $\geq 65\%$ (CR or PR) between T_0 and T_4 was defined as 'response with cytoreduction'.

Thermal imaging was used to assess changes in tumour temperature prior to and over the course of neoadjuvant therapy. Temperature differences between tumoural and non-tumoural areas (TA-NTA) were recorded at different time points (T_1, T_2, T_3 and T_4) and compared to baseline (T_0).

2.7 | Statistical analysis

The Shapiro–Wilk and the Bartlett tests were used to examine the normality of temperature data and confirm the equal variance assumption. Data were not normally distributed and variances were not always equal. Therefore, the Friedman and the Nemenyi post hoc tests were used in the analysis.

Simple regression analysis was conducted to investigate potential correlations between temperature differences and tumour volume. Correlations between tumour volume and temperature differences (TA-NTA) were described using the Spearman correlation coefficient (rho), as follows: high correlation, $r \geq 0.60$; moderate correlation, $0.30 < r < 0.60$; low correlation, $r \leq 0.30$.

The level of statistical significance was set at 5% ($p < 0.05$). Data were managed using Excel (Microsoft Office 365® MSO). Statistical analyses and graph generation and edition were performed using software (RStudio Version 0.99.903, © 2009–2016 RStudio, Inc.).

3 | RESULTS

Epidemiological data and respective tumour characteristics for the dogs with STS ($n = 11$) considered in this study are presented in Table 1. Neoadjuvant therapy with 2-AEH2F was well tolerated and no adverse events were observed during treatment.

Nine out of 11 dogs were submitted to CT at T_0 and T_4. Two patients were unable to perform this exam due to the inoperability of the device. Tomographic image analysis failed to reveal reduction in tumour size in these patients. Therefore, neoadjuvant therapy with 2-AEH2F was not associated with CR or PR (i.e., tumours did not 'respond with cytoreduction') (Figure 1). Tumour size data and respective RECIST, WHO and VOL classifications (CR, PR, PD or SD) are shown in Table 2.

Thermal images were collected from 10 out of 11 dogs at T_0 to T_4. One patient (ID 9) was excluded from the analysis due to missing temperature data (T_{2-4}) (Figure 2). Analysis of temperature differences (TA-NTA) revealed that 'tumours became colder relative to healthy tissue' ($p = 0.01416$) over the course on neoadjuvant therapy (TA-NTA T_{1-4} < TA-NTA T_0) (Table 3). Significant temperature differences were detected between T_0 and T_1 ($p = 0.01802620$), T_0 and T_2 ($p = 0.01409357$) and T_0 and T_3 ($p = 0.03556224$) (Figures 3 and 4). Thermal images depicting temperature differences (TA-NTA) detected over the course of neoadjuvant therapy with 2-AEH2F in patient ID 4 are shown in Figure 5.

3.1 | Correlation between tumour volume and tumour temperature

Correlations between tumour volume (cm^3) and temperature differences (TA-NTA) at time points T_0 to T_3 are shown in Figures 6 and 7, respectively. Temperature differences detected at T_4 were non-significant. Therefore, these data were excluded from the analysis. Moderate to low correlations were detected between these variables ($r = 0.39$). However, these correlations were not significant ($p = 0.2132$).

4 | DISCUSSION

Imaging-based measurement of tumour size pre and post-treatment is the most common method used to investigate tumour response to neoadjuvant chemotherapy in vivo (Stahl et al., 2009). Anatomical models are based on the assumption that tumour shrinkage occurs in response to devitalisation induced by therapy. Tumour shrinkage is thought to be a prerequisite for clinically successful downstaging, that is, establishment of local conditions that facilitate or enable complete surgical resection (Hohenberger & Wysocki, 2008), which is ideal for large-sized or hard-to-reach STSs.

RECIST, WHO and VOL guidelines (one-dimensional, two-dimensional and three-dimensional assessment criteria respectively) are used to evaluate clinical response to treatment in human patients with STS (Grabellus et al., 2012; Stahl et al., 2009). These same guidelines were adopted to evaluate response to therapy in this study. Tomographic measurements failed to reveal complete or partial responses (i.e., tumours did not 'respond with cytoreduction'). Therefore, the potential ability of 2-AEH2F to induce tumour shrinkage reported in experimental studies in mice with melanoma (Ferreira et al., 2011; Veronez, 2012) was not supported by findings of this study.

A major downside of anatomy-based tumour response assessment criteria is the exclusion of functional (biological) changes induced by therapy. This limitation was emphasised in a study with gastrointestinal stromal tumours. In that study, different micro and macroscopic regression patterns, such as necrosis, fibrosclerosis, cystic degeneration and/or haemorrhage, were not taken into account and assessment based on tumour size alone largely underestimated treatment success (Choi et al., 2007).

In a study with non-resectable limb sarcomas submitted to perfusion with TNF-α and melphalan, tumour growth was positively associated with cystic degeneration and/or haemorrhage. The necrotic phenotype of regression prevailed in tumours showing a detectable increase in size after therapy, whereas the fibrosclerotic phenotype was more strongly associated with tumour shrinkage. Anatomy-based (i.e., tumour size) response assessment criteria used in this study were

TABLE 1 Epidemiological data of dogs and tumour characteristics

ID	Sex	Age (y)	Breed dogs	Tumour location	Tumour grade[†]	Mitosis (no. fig-ures/10 HPF)	Percentage of tumour necrosis	Histologic subtypes
4	M	8	Boxer	PL	I	0–1	None	Peripheral nerve sheath tumour
5	F	10	Mixed	Trunk	II	0–9	<50%	Peripheral nerve sheath tumour
6	F	9	Mixed	Gluteus	II	3	<50%	Peripheral nerve sheath tumour
8	F	10	Mixed	PL	I	0–9	None	Peripheral nerve sheath tumour
9	F	11	Mixed	TL	II	0–9	<50%	Peripheral nerve sheath tumour
19	F	9	Mixed	PL	II	2	<50%	—
20	F	6	Mixed	TL	I	2	<50%	Peripheral nerve sheath tumour
21	M	9	German Shepherd	PL	I	0–1	None	—
22	M	9	Belgian Shepherd	PL	I	0–1	None	Peripheral nerve sheath tumour
23	M	…	Mixed	TL	I	0–3	<50%	Peripheral nerve sheath tumour
24	M	13	Maltese	Trunk	I	0–9	None	Fibrosarcoma

[†]Tumour grade determined on the basis of previously described guidelines (Coindre et al., 1988).

ID, patient identification number; M, males; F, females; TL, thoracic limb; PL, pelvic limb; …, unknown data; —, nondescript.
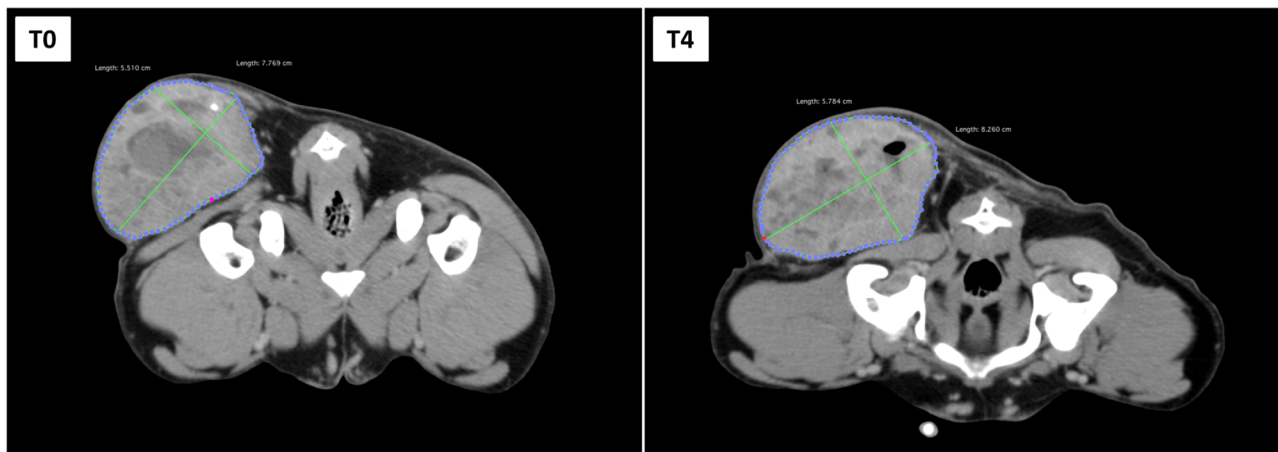

FIGURE 1 Cross-sectional tomographic images of a STS located in the gluteal region (dog ID6). Images were acquired prior to (T_0) and after completion (T_4) of preoperative neoadjuvant therapy with 2-AEH2F. Solid green lines: parameters used for tumour size calculation according to RECIST and WHO criteria (largest tumour diameter and its maximum perpendicular diameter). Dotted blue line: parameter used for tumour volume calculation according to the VOL criterion (tumour outline). Response to therapy in this case was categorised as stable disease according to the three criteria

thought to be accurate enough to discriminate between fibroscle-rotic and necrotic regression phenotypes. Also, fibrosclerosis was more strongly associated with tumour shrinkage than necrosis in this sample. This may be partially explained by the tendency of necrotic tumours to develop cystic changes or cause haemorrhage. Entrapment of serous fluid in non-cystic clefts in extensively necrotic, fluid-filled sarcomas may explain why some highly devitalised tumours increase in size after therapy and support the idea that assessment of clinical response to a given antineoplastic agent should not be based solely on tumour size (Grabellus et al., 2012).

TABLE 2 Values derived from tomographic measurements

| ID	One-dimensional (cm) T_0	One-dimensional (cm) T_4	Increase[†] (%)	RECIST[‡]	Two-dimensional (cm²) T_0	Two-dimensional (cm²) T_4	Increase[†] (%)	WHO[‡]	Volume (cm³) T_0	Volume (cm³) T_4	Increase[†] (%)	VOL[‡]
4	3.75	—	—	—	9.15	—	—	—	19.02	—	—	—
5	8.97	9.46	5.46	SD	63.5973	77.2882	21.53	SD	328.36	403.03	22.74	SD
6	7.76	8.26	6.44	SD	42.7576	47.7428	11.66	SD	193.51	200.85	3.79	SD
8	5.14	6.24	21.40	PD	21.9992	28.3296	28.78	PD	54.05	71.86	32.93	SD
9	4.38	4.84	10.50	SD	15.33	23.958	56.28	PD	47.14	71.43	51.53	PD
19	6.31	7.2	14.10	SD	17.7942	25.344	42.43	PD	48.12	89.52	86.02	PD
20	2.95	3.64	23.38	PD	5.6345	9.3184	65.38	PD	12.20	19.75	61.85	PD
21	6.1	6.65	9.01	SD	32.94	40.0995	21.73	SD	131.64	178.22	35.38	SD
22	3.42	4.06	18.71	SD	7.6266	11.0432	44.80	PD	12.66	23.83	88.19	PD
23	8.75	—	—	—	49.0875	—	—	—	187.81	—	—	—
24	4.69	6.53	39.23	PD	13.0382	27.8178	113.36	PD	46.48	110.01	136.67	PD
Total (n)				SD (n = 6) PD (n = 3)				SD (n = 3) PD (n = 6)				SD (n = 4) PD (n = 5)

[†]Percentage of tumour growth.

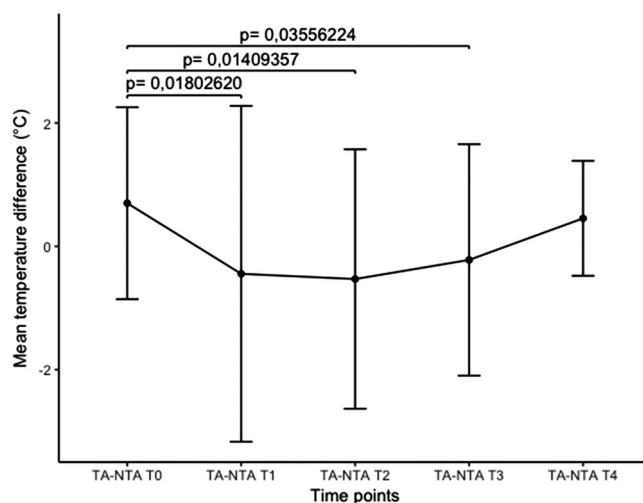[‡]Tumour response assessment criteria.

ID, patient identification number; RECIST, Response Evaluation Criteria in Solid Tumours; WHO, World Health Organization criteria; VOL, volumetric criterion; SD, stable disease; PD, progressive disease; —, not done.

TABLE 3 Temperature differences (mean ± standard deviation) between tumoural (TA) and non-tumoural (NTA) areas

	TA-NTA T_0	TA-NTA T_1	TA-NTA T_2	TA-NTA T_3	TA-NTA T_4	p Value
Temperature (°C)	0.93 ± 1.43	−0.28 ± 2.82	−0.6 ± 2.15	−0.1 ± 1.98	0.58 ± 0.88	0.01416
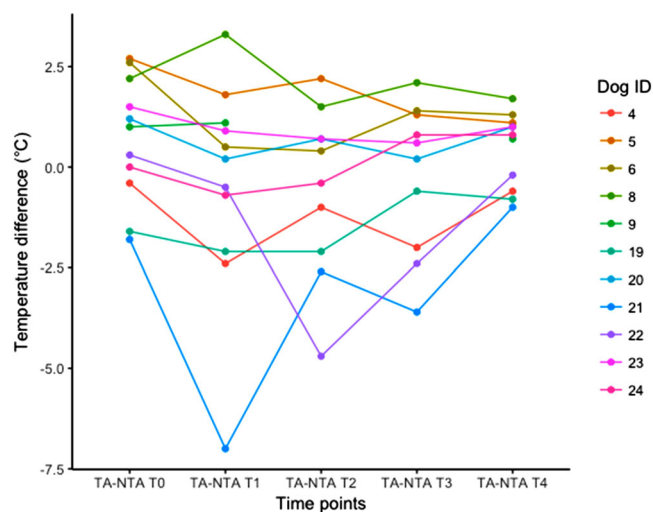
FIGURE 2 Individual behaviour of temperature differences between tumoural and non-tumoural areas (TA-NTA) over the course of neoadjuvant therapy with 2-AEH2F

FIGURE 3 Mean values and standard deviations of temperature differences between tumoural and nontumoural areas (TA-NTA) over the course of neoadjuvant therapy with 2-AEH2F

One of the limitations of our study was that it did not adopt a methodology that might allow us to correlate the histopathological findings (Grabellus et al., 2012), especially the degree of necrosis (Seldon et al., 2021; Weiss et al., 2020), with the changes in tumour size and/or imaging characteristics. Studies in human STS and other malignancies have shown that increasing rates of treatment-induced tumour necrosis correlate with improvement of oncological outcomes and survival. However, the relationship between pathologic response and
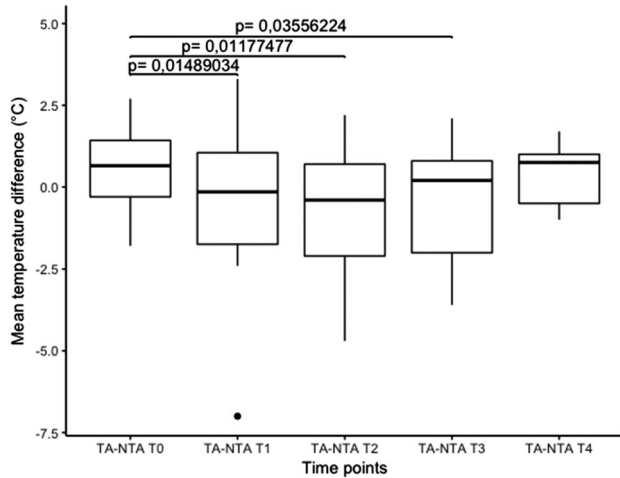
FIGURE 4 Boxplot representing temperature differences between tumoural and non-tumoural areas (TA-NTA) over the course of neoadjuvant therapy with 2-AEH2F

outcomes of specific neoadjuvant treatments for STS remains indeterminate (Seldon et al., 2021).

Physiologic changes may precede anatomical changes commonly detected by radiographic, tomographic or magnetic resonance imaging (Vainionpää, 2014). In a study investigating extracorporeal shock-wave therapy applied to the equine limb, similar findings were derived from thermal and scintigraphic images and both techniques were thought to be sensitive enough to detect physiological changes (Ringer et al., 2005). In this study, thermal imaging revealed a drop in mean temperatures in TA relative to NTA over the course of neoadjuvant therapy with 2-AEH2F. This finding may be explained by several mechanisms: lower metabolic rate and/or decreased tumour blood flow (Van Hoogmoed & Snyder, 2002) and resultant drop in temperature in response to ischaemia or necrosis (Redaelli et al., 2014), tumour cell death in response to toxic changes induced by inflammatory cells (Poljak-Blazi et al., 2009) or poor blood supply typical of fast-growing tumours (Song et al., 2007; Xie et al., 2004).

The impact of sedatives and/or anaesthetic drugs on surface temperature must be accounted for in imaging-based assessment of
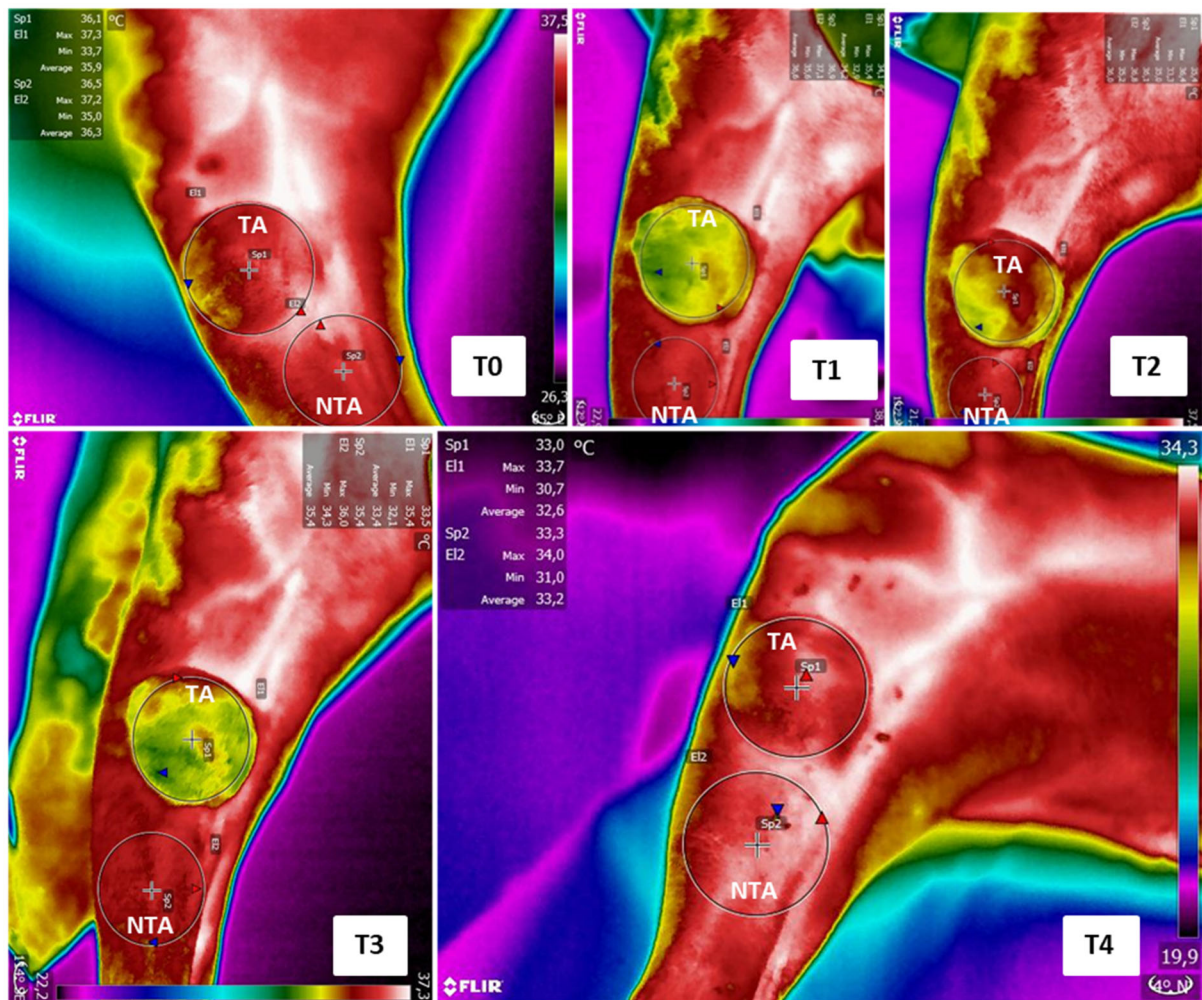

FIGURE 5 Thermal images of the pelvic limb (dog ID6) acquired prior to (T_0) and over the course of (T_1–T_4) neoadjuvant therapy with 2-AEH2F. TA, tumoural area; NTA, non-tumoural área
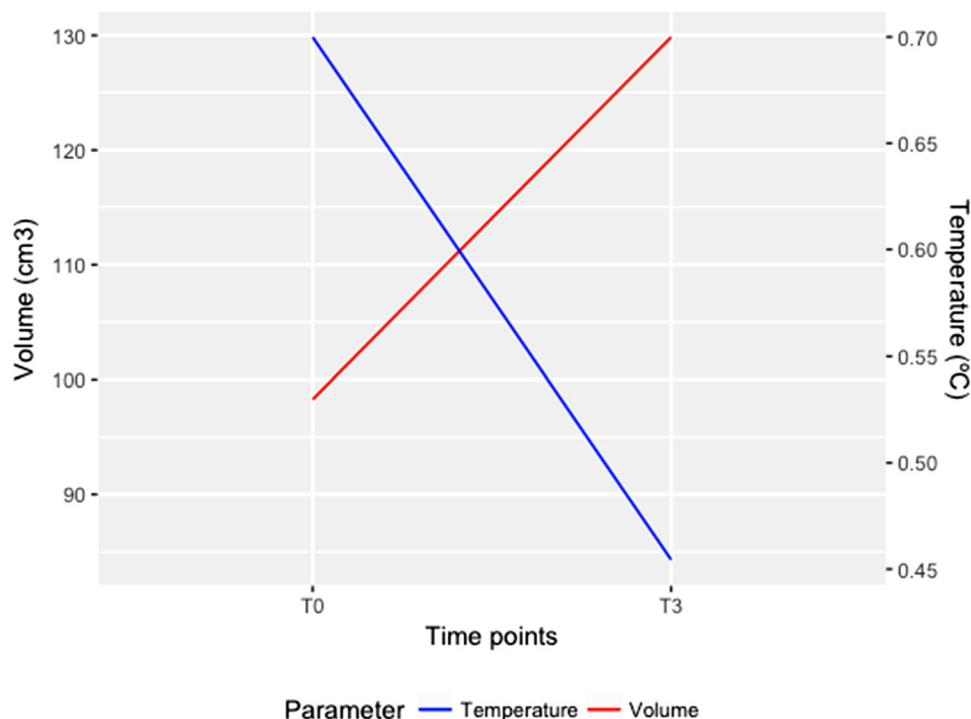
FIGURE 6 Mean values of temperature differences between tumoural and non-tumoural areas (TA-NTA) and tumour volume measured at prior to (T_0) and over the course of (T_3) neoadjuvant therapy with 2-AEH2F
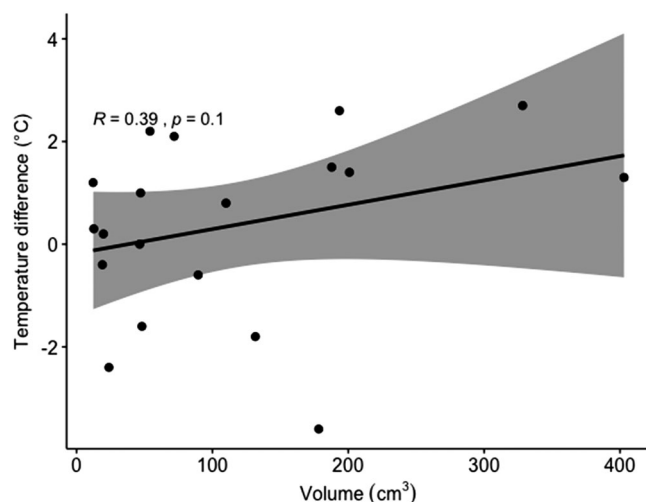

FIGURE 7 Correlations between tumour volume and tumour temperature in dogs undergoing neoadjuvant therapy with 2-AEH2F

sedated or anaesthetised patients (Vainionpää, 2014). In this study, temperatures measured at T_0 were significantly higher relative to T_{1-3}, but not relative to T_4. At this time point (T_4) thermal images were acquired after dogs had been sedated for surgery.

The clinical and experimental applicability of thermal imaging is limited by lack of specificity, given thermal patterns are detected regardless of aetiology (Van Hoogmoed & Snyder, 2002). Hence, lower tumour temperature readings in most patients in this study cannot be attributed exclusively to local effects of 2-AEH2F, such as decreased

intratumoural blood flow and tumour necrosis. In a melanoma study in mice, areas of tumour necrosis increased by approximately 72% following treatment with the highest dose (40 mg/kg) of 2-AEH2F for 20 days, whereas no differences in tumour necrosis were seen after treatment with the lowest dose (10 mg/kg) for 10 days (Veronez, 2012).

In a different study, treatment with 2-AEH2F led to dose-dependent suppression of cell proliferation. At low concentrations, 2-AEH2F activity appears to break the cell cycle at the G2/M phase. In contrast, at high concentration apoptosis is induced. Findings of that study suggest loss of mitochondrial membrane potential and increase in caspase-3 activity suggest 2-AEH2F has dual anti-tumour effect: induction of apoptosis at high concentrations and modulation of cell cycle at low concentrations. In vivo analysis revealed reduced tumour volume and doubling time in mice treated with 2-AEH2F at different concentrations relative to control mice, whereas histologic analysis revealed lower numbers of recently formed fenestrated blood vessels in treated mice and increased formation of similar vessels in control mice. Also, 2-AEH2F-induced changes in cell morphology were typical of apoptosis and tumour shrinkage described in large necrotic areas (Ferreira et al., 2011). Similar changes may have occurred in colder tumoural areas in this study and may be indicative of increased intratumoural necrosis.

Poljak-Blazi et al. (2009) observed reduction of surface temperature at the site of tumour cell inoculation on day 1 and progressive temperature increase as tumour size increased and angiogenesis occurred, with higher temperatures recorded on day 10 and 11 after inoculation. Early temperature drop (i.e., right after tumour implantation) is suggestive of necrosis and may not have been due to insufficient blood

flow in the early stage of tumour development alone, but also to toxic changes induced by inflammatory cells (immune response) and drop in tumour cell count. Dogs in this study may have experienced similar effects, since histologic analysis revealed predominant infiltration of neutrophils and less recently formed vessels in mice with melanoma treated with this phospholipid (Ferreira et al., 2011).

Tumour temperature drop may also reflect poor blood flow in response to rapid tumour growth, as reported by Xie et al. (2004) and Song et al. (2007) in studies with breast cancer cell-derived xenografts in rats. However, rapid growing STSs are uncommon. In fact, these tumours are often slow growing (Stefanello et al., 2008). In this study, tomographic and thermal images revealed that tumours increased in volume and became colder relative to surrounding healthy tissues over the course of treatment with 2-AEH2F, even though correlations between these variables were moderate to low ($r = 0.39$) and non-significant ($p = 0.2132$).

The necrotic regression phenotype prevails in tumours with detectable increase in size after therapy (Grabellus et al., 2012) and physiological changes may precede potential anatomical changes (Vainionpää, 2014). Also, drop in tumour temperature detected using thermal imaging may reflect ischaemia or necrosis (Redaelli et al., 2014). Treatment of melanoma with the lowest dose of 2-AEH2F failed to induce detectable increase in the percentage of necrotic areas compared to higher doses given for longer periods of time in mice (Veronez, 2012). Induction of predominantly neutrophilic infiltration and reduction of recently formed vessels has been reported in mice with melanoma treated with 2-AEH2F at 7 or 14 mg/Kg/intraperitoneal/EDA for 50 days (Ferreira et al., 2011). Administration of 2-AEH2F has been associated with dose-dependent disruption of cell cycle and apoptosis (Ferreira, Meneguelo, Marques et al., 2012). These data suggest weekly intravenous administration of 70 mg/kg doses of 2-AEH2F for four consecutive weeks to dogs with naturally occurring STS in this study was not enough to induce levels of cytotoxicity reported in prior studies (Ferreira, Freitas et al., 2013; Ferreira et al., 2011; Ferreira, Meneguelo, Marques et al., 2012; Ferreira, Meneguelo et al., 2013; Ferreira, Meneguelo, Pereira et al., 2012; Luna et al., 2014; Meneguelo, 2007; Veronez, 2012). However, it may explain physiological changes and resultant surface temperature variations detected on thermal images (Van Hoogmoed & Snyder, 2002) of treated patients (i.e., significant drop in mean TA relative to mean NTA temperature; $p = 0.01416$).

In a Phase-1 study 2-AEH2P was safe at all doses of 150 mg/Kg for 8 weeks in dogs with malignant neoplasms. 2-AEH2P exhibited potent cytotoxic activity against canine primary osteosarcoma and canine breast adenocarcinoma with $IC_{50}\%$ values (De Almeida Leitão Da Cunha et al., 2021). Weekly intravenous administration of the antineoplastic phospholipid 2-AEH2F at 70 mg/kg for four consecutive weeks failed to induce cytoreduction in dogs with naturally occurring STS in this sample. Significant drop in skin temperature in tumoural areas relative to surrounding skin over the course of treatment is consistent with treatment-related physiological or metabolic changes. The natural occurrence of tumours in companion animals is a fundamental strategy for the study of translational medicine drugs used in clinical trials for this species, and also in human patients. 2-AEH2P should be used at doses higher than 70 mg/kg/week in future clinical trials with dogs with naturally occurring neoplasms, and thus continue the investigation of its potential antitumour effect in oncological practice.

ETHICAL STATEMENT

This study was approved by the Ethics Committee on Animal Use (CEUA) of the School of Veterinary Medicine and Animal Science of the University of São Paulo – FMVZ-USP (Protocol: 3495130715/2015). Written informed consent was obtained from dog owners for inclusion in the study.

AUTHOR CONTRIBUTIONS

Patrícia Ferreira de Castro conceived this project, conducted experimental procedures (clinical assessment and surgical procedures), collected data, prepared figures and tables and wrote this manuscript. Durvanei Augusto Maria provided the 2-AEH2F used in this project and contributed to the writing of this manuscript. Ana Carolina Fonseca Brandão de Campos Pinto performed part of tomographic imaging assessments, was responsible for CT image analysis and contributed to the interpretation of CT findings. Geni Cristina Fonseca Patricio anaesthetised the dogs and assisted with data collection. Julia Maria Matera helped to design and coordinate this project and assisted with data interpretation. All authors read and approved the final manuscript.

DATA AVAILABILITY STATEMENT

Datasets presented in the study are available at: https://www.teses.usp.br/teses/disponiveis/10/10137/tde-29112019-120413/

ORCID

Patrícia Ferreira de Castro https://orcid.org/0000-0003-4615-0752

REFERENCES

Borgatti, A., Dickerson, E. B., & Lawrence, J. (2020). Emerging therapeutic approaches for canine sarcomas: Pushing the boundaries beyond the conventional. *Veterinary and Comparative Oncology, 18*(1), 9–24. https://doi.org/10.1111/vco.12554

Brock, N. (1959). Neue experimentelle ergebnisse mit N-lost-phosphamidestern. *Strahlentherapie, 41*:347–354.

Castro, P. F. (2019). Sarcoma de tecidos moles em cães: Tratamento cirúrgico associado à terapia com fosfoetanolamina sintética (FO-S). Published online July 1, 2019 https://doi.org/10.11606/T.10.2020.tde-29112019-120413

Chappell, R., Miranpuri, S. S., & Mehta, M. P. (1998). Dimension in defining tumor response. *Journal of Clinical Oncology, 16*(3), 1234. https://doi.org/10.1200/JCO.1998.16.3.1234

Choi, H., Charnsangavej, C., Faria, S. C., Macapinlac, H. A., Burgess, M. A., Patel, S. R., Chen, L. L., Podoloff, D. A., & Benjamin, R. S. (2007).

Correlation of computed tomography and positron emission tomography in patients with metastatic gastrointestinal stromal tumor treated at a single institution with imatinib mesylate: Proposal of new computed tomography response criteria. *Journal of Clinical Oncology*, 25(13), 1753–1759. https://doi.org/10.1200/JCO.2006.07.3049

Coindre, J.-M., Bui, N. B., Bonichon, F., De Mascarel, I., & Trojani, M. (1988). Histopathologic grading in spindle cell soft tissue sarcomas. *Cancer*, 61(11), 2305–2309.

De Almeida Leitão Da Cunha, O. G., De Sá Rodrigues, L. C., Da Conceição Rabelo, D., Laiso, R. A. N., Chammas, S. M., De Sousa Cabral, L. G., & Maria, D. A. (2021). Clinical oncology translational study phase-1 with antitumor phosphorylethanolamine (2-AEH2P) in dogs with neoplasms. *Journal of Pharmacy and Pharmacology*, 9(5), https://doi.org/10.17265/2328-2150/2021.05.001

Dennis, M. M., Mcsporran, K. D., Bacon, N. J., Schulman, F. Y., Foster, R. A., & Powers, B. E. (2011). Prognostic factors for cutaneous and subcutaneous soft tissue sarcomas in dogs. *Veterinary Pathology*, 48(1), 73–84. https://doi.org/10.1177/0300985810388820

Dernell, W. S., Withrow, S. J., Kuntz, C. A., & Powers, B. E. (1998). Principles of treatment for soft tissue sarcoma. *Clinical Techniques in Small Animal Practice*, 13(1), 59–64.

Ehrhart, N. (2005). Soft-tissue sarcomas in dogs: A review. *Journal of the American Animal Hospital Association*, 41(4), 241–246.

Ferreira, A. K., Freitas, V. M., Levy, D., Ruiz, J. L. M., Bydlowski, S. P., Rici, R. E. G., Filho, O. M. R., Chierice, G. O., & Maria, D. A. (2013). Anti-angiogenic and anti-metastatic activity of synthetic phosphoethanolamine. *PLoS One*, 8(3), e57937. https://doi.org/10.1371/journal.pone.0057937

Ferreira, A. K., Meneguelo, R., Claro Neto, S., Orivaldo Chierice, G., & Augusto Maria, D. (2011). Synthetic phosphoethanolamine induces apoptosis through caspase-3 pathway by decreasing expression of Bax/Bad protein and changes cell cycle in melanoma. *Journal of Cancer Science and Therapy*, 3(3), 53–59. https://doi.org/10.4172/1948-5956.1000058

Ferreira, A. K., Meneguelo, R., Marques, F. L. N., Radin, A., Filho, O. M. R., Neto, S. C., Chierice, G. O., & Maria, D. A. (2012). Synthetic phosphoethanolamine a precursor of membrane phospholipids reduce tumor growth in mice bearing melanoma B16-F10 and in vitro induce apoptosis and arrest in G2/M phase. *Biomedicine & Pharmacotherapy*, 66(7), 541–548. https://doi.org/10.1016/j.biopha.2012.04.008

Ferreira, A. K., Meneguelo, R., Pereira, A., Filho, O. M. R., Chierice, G. O., & Maria, D. A. (2013). Synthetic phosphoethanolamine induces cell cycle arrest and apoptosis in human breast cancer MCF-7 cells through the mitochondrial pathway. *Biomedicine & Pharmacotherapy*, 67(6), 481–487. https://doi.org/10.1016/J.BIOPHA.2013.01.012

Ferreira, A. K., Meneguelo, R., Pereira, A., Mendonça Filho, O. R., Chierice, G. O., & Maria, D. A. (2012). Anticancer effects of synthetic phosphoethanolamine on Ehrlich ascites tumor: An experimental study. *Anticancer Research*, 32(1), 95–104.

Frei, E. (1982). Clinical cancer research: An embattled species. *Cancer*, 50(10), 1979–1992. https://doi.org/10.1002/1097-0142(19821115)50:10<1979::AID-CNCR2820501002>3.0.CO;2-D

Grabellus, F., Stylianou, E., Umutlu, L., Sheu, S-Yi, Lehmann, N., Taeger, G., & Lauenstein, T. C. (2012). Size-based clinical response evaluation is insufficient to assess clinical response of sarcomas treated with isolated limb perfusion with TNF-α and melphalan. *Annals of Surgical Oncology*, 19(11), 3375–3385. https://doi.org/10.1245/s10434-012-2408-1

Hohenberger, P., & Wysocki, W. M. (2008). Neoadjuvant treatment of locally advanced soft tissue sarcoma of the limbs: Which treatment to choose? *The Oncologist*, 13(2), 175–186. https://doi.org/10.1634/theoncologist.2007-0165

Komdeur, R., Hoekstra, H. J., Van Den Berg, E., Molenaar, W. M., Pras, E., De Vries, E. G. E., & Van Der Graaf, W. T. A. (2002). Metastasis in soft tissue sarcomas: Prognostic criteria and treatment perspectives. *Cancer and Metastasis Reviews*, 21(2), 167–183. https://doi.org/10.1023/A:1020893200768

Liptak, J. M., & Christensen, N. I. (2019). Soft tissue sarcomas. In D. M. Vail, D. H. Thamm, & J. M. Liptak (Eds.), *Withrow and MacEwen's small animal clinical oncology* (6th ed., pp. 404–431). W.B. Saunders. https://doi.org/10.1016/B978-0-323-59496-7.00022-0

Lucas, D. R., Kshirsagar, M. P., Biermann, J. S., Hamre, M. R., Thomas, D. G., Schuetze, S. M., & Baker, L. H. (2008). Histologic alterations from neoadjuvant chemotherapy in high-grade extremity soft tissue sarcoma: Clinicopathological correlation. *The Oncologist*, 13(4), 451–458. https://doi.org/10.1634/theoncologist.2007-0220

Luna, A., Agostino, L. G. D., Saraiva, G. K. V., Neto, S. C., Cuccovia, I. M., & Maria, D. A. (2014). The new potential pharmacological of liposomal formulation in tumors. In: A. Méndez-Vilas (Ed.), *Microscopy: Advances in scientific research and education* (pp. 557–563). FORMATEX.

Mauldin, G. N. (1997). Soft tissue sarcomas. *The Veterinary Clinics of North America. Small Animal Practice*, 27(1), 139–148.

Meneguelo, R. (2007). Efeitos antiproliferativos e apoptóticos da fosfoetanolamina sintética no melanoma B16F10. Published online 2007. https://doi.org/10.11606/D.82.2007.tde-12022008-135651

Miller, A. B., Hoogstraten, B., Staquet, M., & Winkler, A. (1981). Reporting results of cancer treatment. *Cancer*, 47(1), 207–214. https://doi.org/10.1002/1097-0142(19810101)47:1<207::AID-CNCR2820470134>3.0.CO;2-6

Poljak-Blazi, M., Kolaric, D., Jaganjac, M., Zarkovic, K., Skala, K., & Zarkovic, N. (2009). Specific thermographic changes during Walker 256 carcinoma development: Differential infrared imaging of tumour, inflammation and haematoma. *Cancer Detection and Prevention*, 32(5–6), 431–436. https://doi.org/10.1016/j.cdp.2009.01.002

Redaelli, V., Tanzi, B., Luzi, F., Stefanello, D., & Proverbio, D. (2014). Use of thermographic imaging in clinical diagnosis of small animal: Preliminary notes. *Annali dell'Istituto Superiore di Sanità*, 50(2), 140–146. https://doi.org/10.4415/ANN

Ringer, S. K., Lischer, C. J., & Ueltschi, G. (2005). Assessment of scintigraphic and thermographic changes after focused extracorporeal shock wave therapy on the origin of the suspensory ligament and the fourth metatarsal bone in horses without lameness. *American Journal of Veterinary Research*, 66(10), 1836–1842.

Seldon, C., Shrivastava, G., Fernandez, M., Jarboe, J., Conway, S., Pretell, J., Freedman, L., Wolfson, A., Zhao, W., Kwon, D., Rosenberg, A., Subhawong, T., Trent, J., & Yechieli, R. (2021). Pathologic response rates after neoadjuvant therapy for sarcoma: A single institution study. *Cancers (Basel)*, 13(5), 1074. https://doi.org/10.3390/cancers13051074

Selting, K. A. (2010). Soft-tissue sarcomas. In C. J. Henry, & M. L. Higginbotham (Eds.), *Cancer management in small animal practice* (p. 403). Saunders.

Song, C., Appleyard, V., Murray, K., Frank, T., Sibbett, W., Cuschieri, A., & Thompson, A. (2007). Thermographic assessment of tumor growth in mouse xenografts. *International Journal of Cancer*, 121(5), 1055–1058. https://doi.org/10.1002/ijc.22808

Sprong, H., Van Der Sluijs, P., & Van Meer, G. (2001). How proteins move lipids and lipids move proteins. *Nature Reviews Molecular Cell Biology*, 2(7), 504–513.

Stahl, R., Wang, T., Lindner, L. H., Abdel-Rahman, S., Santl, M., Reiser, M. F., & Issels, R. D. (2009). Comparison of radiological and pathohistological response to neoadjuvant chemotherapy combined with regional hyperthermia (RHT) and study of response dependence on the applied thermal parameters in patients with soft tissue sarcomas (STS). *International Journal of Hyperthermia*, 25(4), 289–298. https://doi.org/10.1080/02656730902873616

Stefanello, D., Morello, E., Roccabianca, P., Iussich, S., Nassuato, C., Martano, M., Squassino, C., Avallone, G., Romussi, S., & Buracco, P. (2008). Marginal excision of low-grade spindle cell sarcoma of canine extremities: 35 dogs (1996-2006). *Veterinary Surgery*, 37(5), 461–465. https://doi.org/10.1111/j.1532-950X.2008.00408.x

Therasse, P., Arbuck, S. G., Eisenhauer, E. A., Wanders, J., Kaplan, R. S., Rubinstein, L., Verweij, J., Van Glabbeke, M., Van Oosterom, A. T., Christian, M.

C., & Gwyther, S. G. (2000). New guidelines to evaluate the response to treatment in solid tumors. *Journal of the National Cancer Institute*, *92*(3), 205–216. https://doi.org/10.1093/jnci/92.3.205

Thrall, D. E., & Gillette, E. L. (1995). Soft-tissue sarcomas. *Seminars in Veterinary Medicine and Surgery (Small Animal)*, *10*(3), 173–179.

Vainionpää, M. (2014). Thermographic imaging in cats and dogs usability as a clinical method. Published online 2014. Accessed March 15, 2019. https://core.ac.uk/download/pdf/20441286.pdf

Van Blitterswijk, W. J., & Verheij, M. (2013). Anticancer mechanisms and clinical application of alkylphospholipids. *Biochimica et Biophysica Acta (BBA) – Molecular and Cell Biology of Lipids*, *1831*(3), 663–674. https://doi.org/10.1016/j.bbalip.2012.10.008

Van Der Luit, A. H., Budde, M., Verheij, M., & Van BLITTERSWIJK, W. J. (2003). Different modes of internalization of apoptotic alkyl-lysophospholipid and cell-rescuing lysophosphatidylcholine. *Biochemical Journal*, *374*(3), 747–753. https://doi.org/10.1042/BJ20030179

Van Der Luit, A. H., Vink, S. R., Klarenbeek, J. B., Perrissoud, D., Solary, E., Verheij, M., & Van Blitterswijk, W. J. (2007). A new class of anticancer alkylphospholipids uses lipid rafts as membrane gateways to induce apoptosis in lymphoma cells. *Molecular Cancer Therapeutics*, *6*(8), 2337–2345. https://doi.org/10.1158/1535-7163.MCT-07-0202

Van Hoogmoed, L. M., & Snyder, J. R. (2002). Use of infrared thermography to detect injections and palmar digital neurectomy in horses. *Veterinary Journal*, *164*(2), 129–141. https://doi.org/10.1053/TVJL.2002.0719

Veterinary cooperative oncology group – Common terminology criteria for adverse events (VCOG-CTCAE) following chemotherapy or biological antineoplastic therapy in dogs and cats v1.1 (2016). *Veterinary and Comparative Oncology*, *14*(4), 417–446. https://doi.org/10.1111/vco.283

Veronez, L. C. (2012). Atividade Da Fosfoetanolamina Sintética Em Melanoma Murino Experimental. Published online 2012:80. https://doi.org/10.11606/D.17.2012.tde-15122012-123717

Weiss, A. R., Chen, Y.-L., Scharschmidt, T. J., Chi, Y.-Y., Tian, J., Black, J. O., Davis, J. L., Fanburg-Smith, J. C., Zambrano, E., Anderson, J., Arens, R., Binitie, O., Choy, E., Davis, J. W., Hayes-Jordan, A., Kao, S. C., Kayton, M. L., Kessel, S., Lim, R., …Wang, D. (2020). Pathological response in children and adults with large unresected intermediate-grade or high-grade soft tissue sarcoma receiving preoperative chemoradiotherapy with or without pazopanib (ARST1321): A multicentre, randomised, open-label, phase 2 trial. *The Lancet Oncology*, *21*(8), 1110–1122. https://doi.org/10.1016/S1470-2045(20)30325-9

Xie, W., Mccahon, P., Jakobsen, K., & Parish, C. (2004). Evaluation of the ability of digital infrared imaging to detect vascular changes in experimental animal tumours. *International Journal of Cancer*, *108*(5), 790–794. https://doi.org/10.1002/ijc.11618